ARTICLE IN PRESS

Available online at www.sciencedirect.com

SCIENCE DIRECT®

MICROPOROUS AND MESOPOROUS MATERIALS

ELSEVIER

Microporous and Mesoporous Materials 79 (2005) 171–175

www.elsevier.com/locate/micromeso

Ion exchange of Cu^{2+}, Ni^{2+}, Pb^{2+} and Zn^{2+} in analcime (ANA) synthesized from Thai perlite

Sudaporn Tangkawanit [a,1], Kunwadee Rangsriwatananon [a], Alan Dyer [b,*]

[a] *School of Chemistry, Institute of Science, Suranaree University of Technology, Nakorn Ratchasima, 30000, Thailand*
[b] *Institute of Materials Research, University of Salford, Cockcroft Building, Salford M5 4WT, UK*

Received 10 August 2004; accepted 31 October 2004

Abstract

This work studied the ion exchange of Cu^{2+}, Ni^{2+}, Pb^{2+} and Zn^{2+} into an analcime (ANA) in the temperature range 298–333 K. The analcime was produced from an economically available Thai perlite. The selectivity sequence for ions entering analcime in its as-synthesized sodium form was $Pb^{2+} > Cu^{2+} > Zn^{2+} > Ni^{2+}$, as indicated by values of ΔG^0. The results demonstrated that the enthalpy of cation hydration determined the selectivity of the zeolite. ΔS^0 values were related to changes in water content. A comparison of the selectivity series for Pb, Cu, Ni, and Zn cation uptake into analcime to those of other zeolites shows similar trends.

Keywords: Ion exchange; Perlite; Analcime; Heavy metals; Selectivity, Thermodynamic parameters

1. Introduction

The analcime (ANA) structure is made up of linked tetrahedral units proscribing three non-connected channels [1]. Small pore zeolites, such as analcime, can constitute a basis for possible future technical innovations in selective adsorption and heterogeneous catalysis [2]. Analcime has pore openings of 2.6 Å and maximum cation exchange capacity 4.9 meq g^{-1} [3]. Barrer and Townsend found that, when transition metals exchange into the sodium zeolites A, X and Y, the more siliceous the zeolite the less favoured is exchange of the sodium by Co^{2+}, Ni^{2+}, Cu^{2+} and Zn^{2+} [4]. In an exchange of a pair of ions, the larger cation is preferred by the zeolite with *lower framework charge (high Si/Al) and the smaller cation* by a framework with higher charge (low Si/Al) [5].

Ion exchange isotherms in analcime have been reported for K, Tl, Rb, NH_4 and Ag, by Barrer and Hinds [6]. Barrer also noted that the very small Li^+ cation did not readily exchange due to its high energy of hydration in solution [7]. Balgord and Roy [8] reported that Na-analcime can be completely exchanged by K^+, Ag^+, Tl^+, NH_4^+ and Rb^+ cations at elevated temperatures, whereas only small amounts of Sr, Mg, Ni and Co move into analcime.

In this work, analcime synthesized from Thai perlite was examined for its potential use as an ion exchanger for removal of the toxic metals Cu^{2+}, Ni^{2+}, Pb^{2+} and Zn^{2+}.

2. Experimental

2.1. Synthesis

Analcime was synthesized from economically available perlite (volcanic glass) collected from Lopburi

* Corresponding author. Tel.: +44 01254 761 384.
E-mail addresses: tangkawa@yahoo.com (S. Tangkawanit), aldilp@aol.com (A. Dyer).
[1] Present Address: Department of Chemistry, Faculty of Science and Technology, Ubon Ratchatani Rajabhat University, Ubon Ratchatani, 34000, Thailand.

1387-1811/$ - see front matter © 2004 Elsevier Inc. All rights reserved.
doi:10.1016/j.micromeso.2004.10.040

2. Experimental

2.1. Synthesis

Analcime was synthesized from perlite collected from Lopburi Province in central Thailand. Perlite was ground to pass through a 230 mesh and then reacted with 3M NaOH (w/v of 1:5 solid to liquid), at 413K for 24h in a 500ml high-pressure/high-temperature stirred reactor (Parr Instruments). After hydrothermal treatment, the products were filtered, washed with deionised water, and dried for 6h at 393K.

2.2. Characterisation of analcime

The chemical compositions (Table 1) of raw perlite and its analcime product were determined by wavelength dispersive X-ray fluorescence spectrophotometer (XRF), (Model Negitive Magix Pro, Phillips).

The analcime was further characterized by X-ray diffraction (XRD) using a Bruker, D5005 instrument. Silicon–aluminum ordering was characterized by MAS NMR using a Varian Unity Inova spectrometer, at a frequency of 59.58MHz, and used to calculate the Si/Al ratio in the normal way (D. Apperley, University of Durham, UK). The spectra were recorded with a spinning rate of 6kHz in a Varian 5.0mm MAS probe, at ambient temperature. XRD, ^{29}Si MAS NMR traces and the SEM (Model JSM6400, JEOL) of the analcime are presented in Fig. 1.

Water content and thermal stability of the analcime were examined by heating 10mg of analcime at 10K/min, in a flow of dry nitrogen, using a thermal analyser (TGA-DTA), SDT 2960. Particle size analysis was carried out, after grinding in an agate mortar, using a laser particle size analyzer Malvern Instruments Mastersizer S.

Determination of the cation exchange capacity (CEC) was carried out by isotope dilution analysis. Analcime samples (0.1g) were weighed into plastic containers, and equilibrated with 20ml 0.01M ^{22}Na nitrate (supplied by Amersham International, UK) in a thermostatically controlled air oven until equilibrium was reached (two days). The activities in the liquid phase were measured before and after equilibration by liquid scintillation counting. BET nitrogen surface areas were determined

Table 1
Chemical composition (wt%) of raw perlite and synthetic analcime

Oxide	Perlite	Analcime
SiO_2	70.63	52.44
Al_2O_3	13.10	24.30
K_2O	4.71	0.34
Na_2O	2.36	12.53
CaO	0.48	0.28
Fe_2O_3	1.49	1.61
MgO	0.90	–
TiO_2	0.24	–
MnO_2	0.03	–
H_2O	3.5	8.5
Total	95.5	100

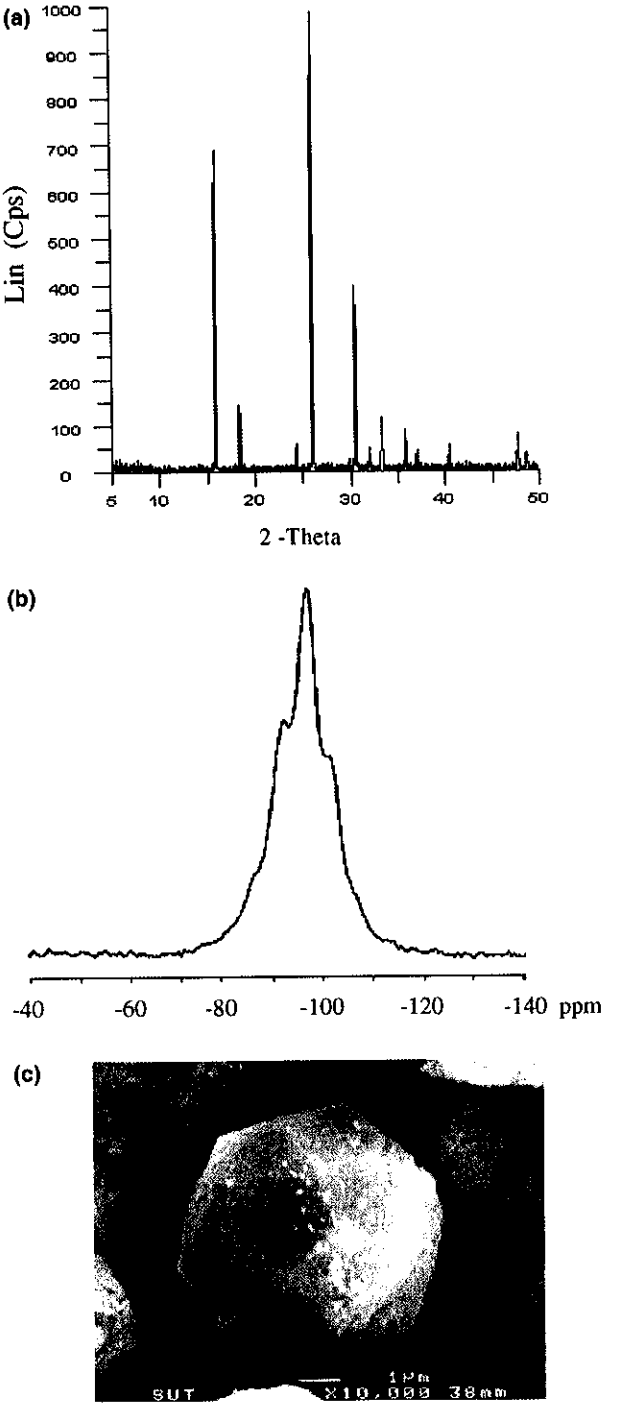

Fig. 1. Characterisation of synthetic analcime prepared from Thai perlite (a) XRD diffractrogram, (b) ^{29}Si MAS NMR spectra and (c) SEM photograph.

Table 2
Properties of raw perlite and synthetic analcime

	Perlite	Analcime
BET surface area	15.85 m^2/g	18.92 m^2/g
CEC	–	4.16 meq g^{-1}
Si/Al (MAS NMR)	–	1.97
Particle diameter	3.20 μm	7.75 μm

by using a Micrometrics model ASAP 2010. Table 2 summarizes the results of these measurements.

Fully exchanged forms of analcime were also prepared by using Cu, Ni, Pb and Zn 0.5 M nitrate solutions (Merck analytical grade). Duplicate exchanges were carried out, changing solutions twice a day for seven days. X-ray powder diffraction was used to confirm the retention of crystallinity in the solid phase after exchange.

2.3. Diffusion experiments

The analcime was pre-labeled with a known activity of ^{22}Na. Diffusion of heavy metal cations into analcime was studied by contacting 0.1 g of ^{22}Na analcime with 5 ml 0.01 M solution of the in-going cation in plastic vials. The vials were rotated about their horizontal axes, in a thermostatically controlled air oven, for various times between 0.5 and 24 h. At the end of appropriate time periods the plastic containers were taken from the oven and immediately centrifuged. The extents of heavy metal cation diffusion into analcime were measured from the release of ^{22}Na into solution, as determined by liquid scintillation counting. Kinetic plots were constructed at 298, 313 and 333 K.

2.4. Diffusion kinetics

Barrer et al. [11] suggest the following equation for the estimation of diffusion coefficients (D), taken to be independent of the concentration and in the absence of surface barriers, for crystals of uniform size and approximated as spheres of radius r_0:

$$I_0 = \int_0^\infty \left(1 - \frac{w_t}{w_\infty}\right) dt = \frac{r_0^2}{15D} \quad (1)$$

where I_0 is the area between the asymptote and the kinetic curve, W_t and W_∞ are, respectively, the extents of exchange at time $t = t$, and $t = \infty$.

The activation energy can be evaluated by using the Arrhenius equation:

$$D = D_0 e^{-E_a/RT} \quad (2)$$

where E_a is the activation energy; and R the gas constant. A plot of $\ln D$ against reciprocal temperature T (K^{-1}) yields a straight line of slope—E_a/R. The entropy of activation can be calculated from Eq. (3), which is taken from Refs. [5,12]:

$$D_0 = 2.72(kTd^2/h)\exp(\Delta S^*/R) \quad (3)$$

where k and h are the Boltzmann and Planck constants, respectively; d is the inter-ionic jump distance between adjacent sites. This was assumed to be 0.76 nm [5]. D_0 is a pre-exponential factor representing the hypothetical diffusion coefficient at absolute zero. Other thermodynamic parameters were calculated in the normal manner (note, $E_a = \Delta H^* + RT$).

3. Results and discussion

3.1. Characterisation

The analcime XRD pattern (Fig. 1) matched that of literature values, and confirmed it to be essentially pure. XRF and MAS NMR confirmed an empirical formula close to that of natural analcimes [13]. MAS NMR spectra obtained at both a 5 s and a 60 s recycle were consistent. Relatively intense spinning side bands were noted (not shown). These, with the relatively broader centre band signals, can be accounted for by the known iron content (Table 1). The surface area was similar to previous measurements on a synthetic analcime [14]. The SEM showed the analcime crystallites to have the typical icositetrahedral habit of this zeolite. Concerning the particle site distribution see Fig. 2.

Thermograms of the synthetic analcime are shown in Fig. 3. The zeolite had a total mass loss of 8.5%, like the value of 8.4% due to water loss quoted in previous work [15]. DTA showed the typical endothermic dehydration curve of analcime in the range 473–673 K. The trace also showed that the structure of analcime was stable to at least 1073 K.

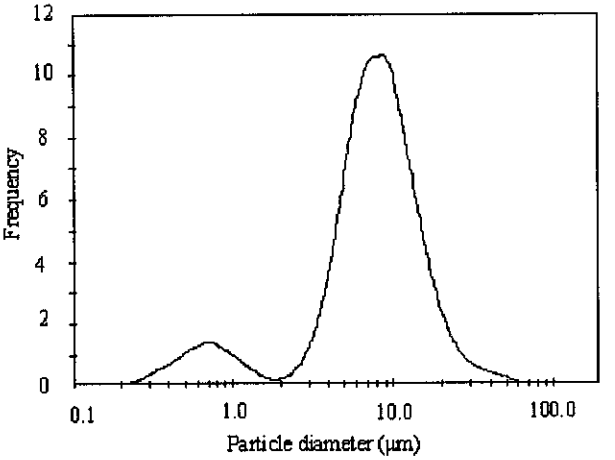

Fig. 2. Particle size distribution of analcime crystallites.

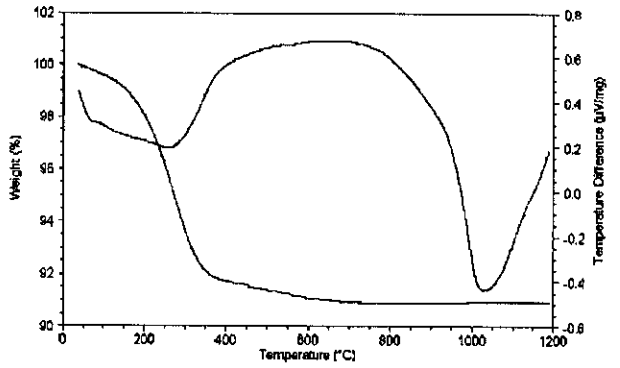

Fig. 3. TGA-DTA thermograms of a synthetic analcime sample.

The XRD d-spacings of the fully exchanged analcimes, prepared separately, showed minor variations coupled with small intensities changes. These were to be expected from ingress of cations with differing X-ray absorption coefficients and sizes. The baselines of their XRD patterns, however, remained almost linear. Fig. 3a shows a plot of percentage crystallinity against cation radius. Taking into account the possible loss in pattern intensity caused by the presence of metals other than sodium, several treatments with 0.5 M excess of in-going cations resulted in only a 2–10% decrease in observed crystallinity. This confirmed that the structure of analcime will remain unchanged during diffusion studies carried out using 0.01 M solutions.

3.2. Diffusion measurements

The habit of the analcime crystallites is sufficiently close to spherical to justify the use of Eq. (1), but the particle size distribution is clearly bimodal (Fig. 2). This means that the D-values observed are average values, but can be used to compare the performance of the analcime synthesized from the natural perlite source.

The W_t/W_∞ plots for diffusion processes are shown in Figs. 4–7. Their shapes and the evident large temperature coefficients suggest that the kinetics are controlled by intracrystalline diffusion, and are not affected by the presence of surface barrier layers. Plots of $\ln D$ against $1/T$ were of good linearity (Figs. 8 and 9).

Table 3 shows the thermodynamic parameters for the diffusion of cations into Na analcime at different temperatures. Exchange diffusion coefficients for Cu^{2+}, Ni^{2+}, Pb^{2+} and Zn^{2+} in analcime are of the order of $10^{-17}m^2s^{-1}$. This is consistent with previous work that found sodium and potassium self-diffusion coefficients in analcime to be 10^{-16}–$10^{-17}m^2s^{-1}$ at 293 K [16].

The free energies of exchange confirm that similar processes are being followed for the different cations and, again, are of the same order of magnitude as those measured for Na and K self-diffusion in analcime [5] (Fig. 10).

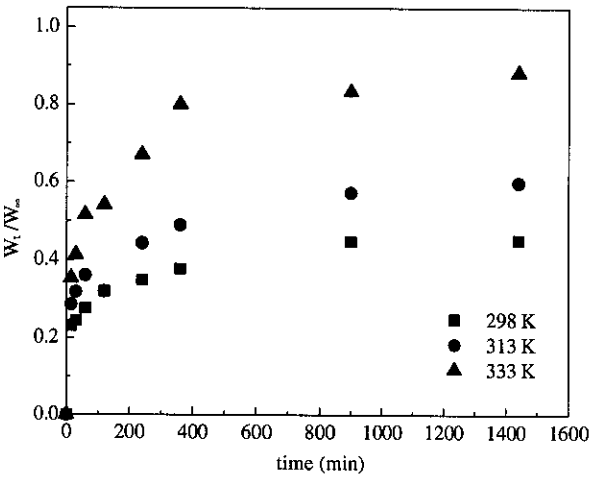

Fig. 4. Plots of W_t/W_∞ against time (t) for $^{22}Na/\frac{1}{2}Cu^{2+}$ exchange in analcime, in the range 298–333 K.

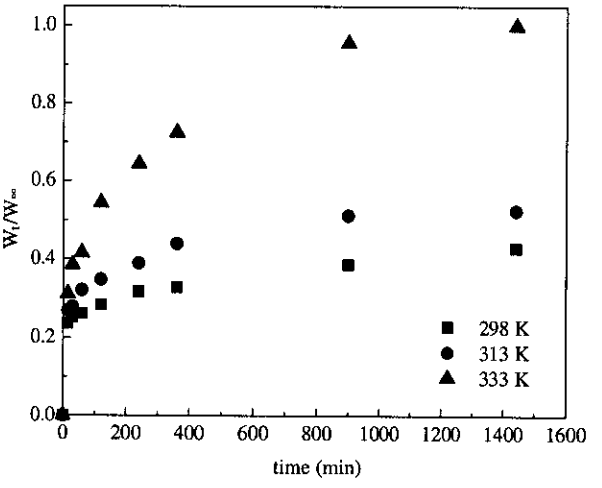

Fig. 5. Plots of W_t/W_∞ against time (t) for $^{22}Na/\frac{1}{2}Ni^{2+}$ exchange in analcime, in the range 298–333 K.

Values for the energies of activation for the cation exchanges follow the series Zn < Cu < Pb < Ni, and recourse to Fig. 11 shows that the value recorded for lead is lower than expected from its bare ion size. This reflects the polarisability of the Pb cation, i.e., it can "squeeze" into the narrow analcime channels more readily than would be expected from its size. The order of the activation energies for the other cations follows that of bare cation size, coupled with d electron shells, so it seems that the waters of hydration are lost prior to migration into the analcime structure. The activation energies are, in general, lower than those encountered by sodium and potassium cations as they move through the analcime structure, which is in accord with their larger and less hydrated cations. Similarly entropy changes for sodium and potassium self-diffusion processes in analcime are less negative than those measured herein.

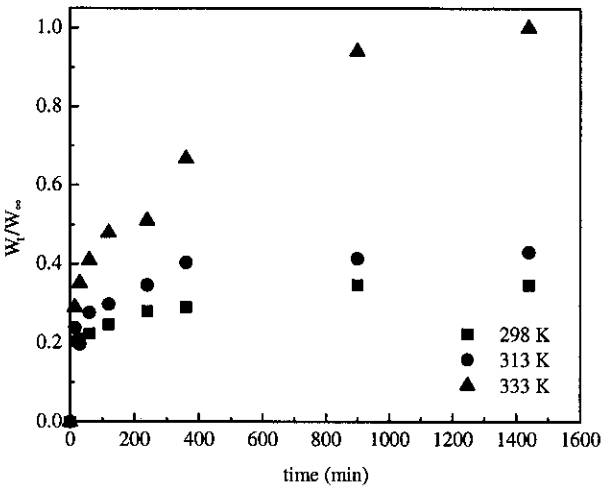

Fig. 6. Kinetic plots of W_t/W_∞ against time (t) for $^{22}Na/\frac{1}{2}Pb^{2+}$ exchange in analcime, in the range 298–333 K.

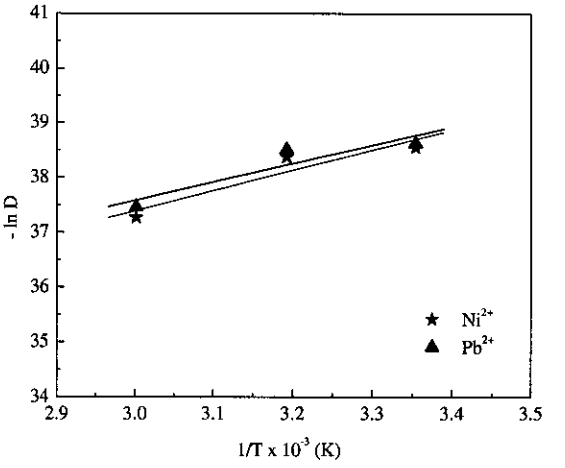

Fig. 8. Arrhenius plots for exchange diffusion of Ni^{2+} and Pb^{2+} in analcime, in the range 298–333 K.

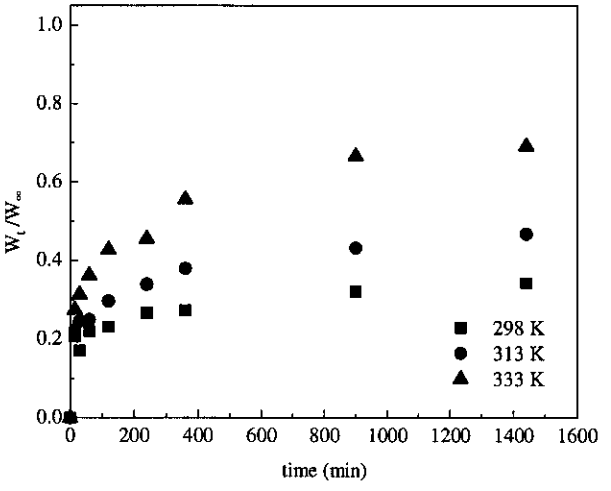

Fig. 7. Kinetic plots of W_t/W_∞ against time (t) for $^{22}Na/\frac{1}{2}Zn^{2+}$ exchange in analcime, in the range 298–333 K.

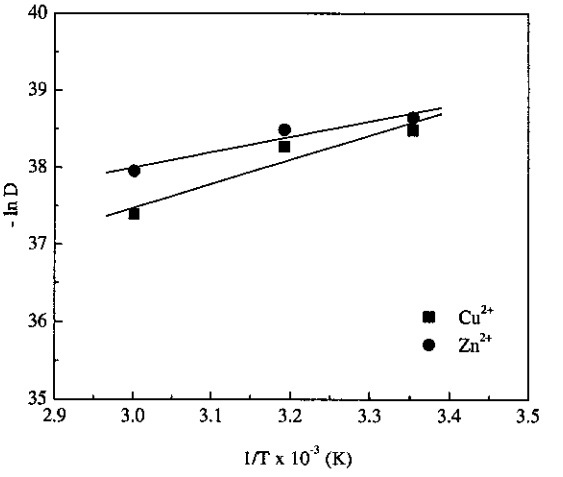

Fig. 9. Arrhenius plots for exchange diffusion of Cu^{2+} and Zn^{2+} in analcime in the range 298–333 K.

Table 3
Thermodynamic parameters for the diffusion of cations into Na-analcime

Cation	Temperature (K)	E_a (kJ mol^{-1})	ΔS^* (JK^{-1} mol^{-1})	ΔH^* (kJ mol^{-1})	ΔG^* (kJ mol^{-1})
Cu^{2+}	298	26.2	−136	23.7	64.5
	313		−137		66.6
	333		−138		69.3
Ni^{2+}	298	30.8	−122	28.3	64.5
	313		−123		66.6
	333		−124		69.3
Pb^{2+}	298	28	−132	25.4	65.0
	313		−133		66.0
	333		−134		69.6.
Zn^{2+}	298	17	−169	14.2	64.8
	313		−170		67.4
	333		−171		70.8

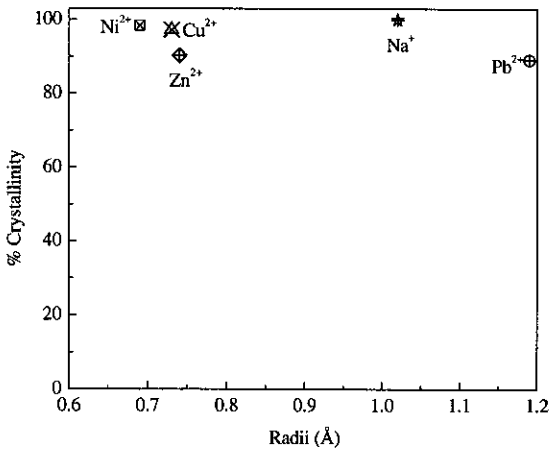

Fig. 10. Plot of % crystallinity against cation radii for cation exchanged analcimes.

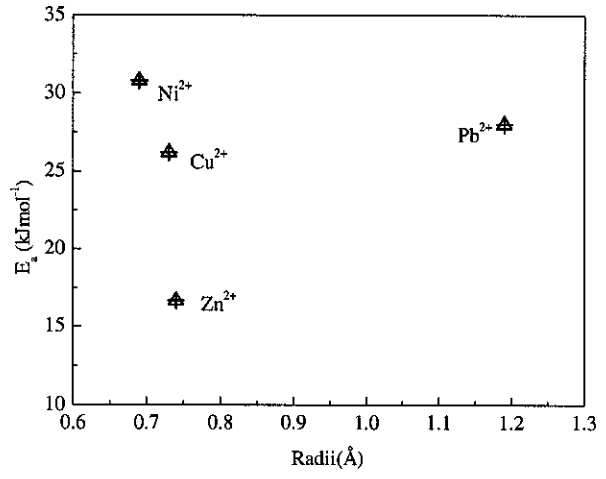

Fig. 11. Plot of the activation energy (E_a) against cation radii for diffusion processes.

This reflects the replacement of two monovalent ions by one divalent ion in the available zeolite cation sites in this work. The correlation between the activation energy and activation entropy values illustrates the "compensation effect" commonly seen in diffusion phenomena. Differences in ΔS^* values could thus reflect systematic differences in the potential energy terrain encountered by the diffusing cations in the zeolite (correlation between the height of the energy barrier and the curvature of the energy at the barrier) [17].

The extents of exchange seen in Figs. 4–7 suggest that all exchange sites in analcime structure are available to the in-going cations, in the temperature range studied, apart from when zinc is considered. It seems that, up to 333 K, only sites in two of the three channels are taken up by zinc. This may arise from a size restriction caused by zinc moving as a partially hydrated cation thus hindering its progress into the smallest channel of the analcime structure. Support for this concept comes from the relatively lower change in activation entropy noted in the sodium for zinc exchange (Table 3).

Comparison to thermodynamic diffusional parameters measured for cation exchanges in clinoptilolite [3], using the BBK (Barrer, Barri and Klinowski) equation, show that exchanges in this zeolite are more facile ($\Delta G^* = 29$–48 kJ mol^{-1} for Na/NH_4, K/Na, and Na/$\frac{1}{2}$Ca ion pairs in clinoptilolite). Energy barriers fall in the range 17–42 kJ mol^{-1}, and changes in entropy are much lower than those measured here, as expected from relatively unhydrated cations moving through the clinoptilolite framework.

4. Conclusions

Perlite has proved to be a successful source material for the synthesis of a pure analcime, which acts as a potentially useful material for the uptake of heavy metals from aqueous solution.

The energy barriers to cation movements into the zeolite framework represent movements of bare ions into analcime, except for zinc, which may ingress as a partially hydrated moiety. Although lead is the largest ion studied it is able to enter the narrow analcime structure, because of its high polarisability.

Acknowledgments

We wish to thank Dr. David Apperley, University of Durham, UK, for his excellent MAS NMR service. Sudaporn Tangkawanit would like to thank Rajabhat Ubon Ratchatani University for financial support for the part of this work that was carried out at the University of Salford. Thanks are due to the helpful suggestions provided by the referees.

References

[1] A. Dyer, An Introduction to Zeolite Molecular Sieves, John Wiley and Son, Chichester, UK, 1988, pp.73–74.
[2] D. Kallo, Natural zeolites: occurrences, properties, applications, in: D.L. Bish, D.W. Ming (Eds.), Reviews in Mineralogy and Geochemistry, Vol. 45, Mineralogical Society of America, Washington, DC, 2001, p. 519.
[3] A. Dyer, K.J. White, Thermochim. Acta 340–341 (1999) 341.
[4] P. Yang, J. Stolz, J.T. Armbuster, M. Gunter, Am. Mineral. 82 (1997) 517.
[5] A. Dyer, A.M. Yusof, Zeolites 7 (1987) 196.
[6] W.M. Meier, D.H. Olson, Ch. Baerlocher, Atlas of Zeolite Structure Types, fourth ed., Butterworth-Heinemann, Stoneham, MA, 1996, pp. 42–43.
[7] P. Saha, Am. Mineral. 44 (1959) 300.
[8] W.D. Balgord, R. Roy, in: Molecular Sieve Zeolites-1Advances in Chemistry, 101, American Chemical Society, Washington, DC, 1971, p. 140.
[9] R.M. Barrer, J. Chem. Soc. (1950) 2342.
[10] A. Dyer, A.M. Yusof, Zeolites 9 (1989) 129.

[11] R.M. Barrer, S.A.I. Barri, J. Klinowski, J. Chem. Soc. Faraday Trans. 1 (76) (1980) 1038.
[12] R.M. Barrer, R.F. Bartholomew, L.V.C. Rees, J. Phys. Chem. Solids 21 (1961) 12.
[13] G. Gottardi, E. Galli, Natural Zeolites, Springer-Verlag, Berlin Heidelberg, 1985, p. 82.
[14] A. Molyneux, Ph.D. Thesis, University of Salford, 1967.
[15] M. Todorovic, Z. Radak-Jovanovic, I.J. Gal, A. Dyer, Colloids Surf. Sci. 23 (1987) 350.
[16] A.M. Yusof, Ph.D. Thesis, University of Salford, 1984.
[17] Suggestion from a referee.